Room temperature sub-bandgap photoluminescence from silicon containing oxide precipitates

K. Bothe,[1,a)] R. J. Falster,[2,3,b)] and J. D. Murphy[3,c)]
[1]*Institut für Solarenergieforschung Hameln/Emmerthal, Am Ohrberg 1, 31860 Emmerthal, Germany*
[2]*MEMC Electronic Materials, viale Gherzi 31, 28100 Novara, Italy*
[3]*Department of Materials, University of Oxford, Parks Road, Oxford OX1 3PH, United Kingdom*

(Received 9 February 2012; accepted 28 June 2012; published online 19 July 2012)

Room temperature photoluminescence was measured from p-type Czochralski silicon processed to contain oxide precipitates. No detectable luminescence was associated with unstrained oxide precipitates. Strained oxide precipitates gave rise to a broad luminescence peak centred at ~1600 nm. The intensity of the peak increased with the density of strained precipitates, with band-to-band luminescence being reduced correspondingly. Dislocations and stacking faults around the strained precipitates were found to introduce competing non-radiative recombination centres which reduced the sub-bandgap photoluminescence. A mechanism is proposed for the sub-bandgap luminescence due to strained precipitates in terms of a transition between defect bands. © *2012 American Institute of Physics*. [http://dx.doi.org/10.1063/1.4737175]

Single crystal Czochralski silicon (Cz-Si) is the material of choice for most microelectronic applications. Cast multicrystalline silicon (mc-Si) and Cz-Si are also used for ~90% of photovoltaics (PV). Both materials have a high interstitial oxygen content (~10^{17} to 10^{18} cm^{-3}), arising from the dissolution of the melt-containing silica crucible. In Cz-Si for microelectronics, intentional high temperature annealing is often used to form oxide precipitates to act as sinks for mobile transition metal impurities as part of internal gettering processes.[1] Unintentional precipitation of oxygen occurs during the casting of mc-Si (Refs. 2–4) and in rapidly pulled Cz-Si crystals used for PV.[5,6] Oxide precipitates are strong recombination centres,[7–10] so have a significant detrimental impact on solar cell efficiencies.[5,11]

Oxide precipitates are known to undergo a morphological transformation during growth.[12,13] In the early stages of oxygen precipitation unstrained precipitates are believed to form.[13] Undetectable by etching and transmission electron microscopy (TEM), their existence is inferred from oxygen-loss experiments.[13] These change morphology into a strained state as they grow, becoming detectable by etching and TEM (Refs. 12 and 13) and active for gettering.[13] Dislocations and stacking faults form around the precipitates with further processing. Our recent work has shown the recombination activity of the defects is relatively weak at unstrained precipitates, stronger at strained precipitates, and stronger still when the strained precipitates are surrounded by dislocations and stacking faults.[8,10]

As an indirect gap semiconductor, silicon does not emit light very efficiently. However, weak radiative recombination can occur via band-to-band processes and via defect states within the bandgap. A wide variety of photoluminescence (PL) signals have been associated with oxygen-related defects in silicon.[3,14–22] At room temperature, oxide precipitates give rise to a broad PL peak at ~0.8 eV.[3,16,18] At first glance, this could be attributed to dislocation-related PL D-lines found at liquid helium temperatures,[23] but Tajima *et al.* have used microscopic PL mapping to show this defect band is instead associated with oxygen precipitation.[3,18]

In this Letter, we present room temperature spectrally resolved PL results for Cz-Si samples processed to contain oxide precipitates. Samples were prepared from 150 mm diameter high-purity Cz-Si wafers with a boron doping concentration of $(1.3 \pm 0.2) \times 10^{15}$ cm^{-3}. Fourier transform infrared (FTIR) spectroscopy gave the initial interstitial oxygen concentrations as $(7.7 \pm 0.2) \times 10^{17}$ cm^{-3} (DIN 50438-1). The carbon content was below the FTIR detection limit of 5×10^{15} cm^{-3}. Wafers were subjected to a four-stage precipitation treatment:[24] (i) homogenization anneal at 1000 °C for 15 min to dissolve grown-in precipitates; (ii) nucleation anneal at 650 °C for 6 to 32 h to create precipitate nuclei with different densities; (iii) "drift" anneal at 800 °C for 4 h shifting the distribution of nuclei with clusters larger than the critical size at 800 °C to sizes sufficiently large to survive a 1000 °C anneal; and (iv) growth anneal at 1000 °C for 0.5 to 16 h. The procedure yielded a matrix of 24 wafers with nucleation times ranging from 6 to 32 h and growth times between 0.5 to 16 h (Fig. 1). Great care was taken to avoid impurity contamination during processing. The bulk iron concentration was measured by photodissociation of iron-boron pairs[8,25] in each processed sample and was always less than 4×10^{11} cm^{-3} (plotted in Ref. 8).

The density of strained precipitates was determined by Schimmel etching of a cleaved edge of material taken from a position in a wafer immediately adjacent to the 4×5 cm^2 PL sample. The density of strained precipitates increases with growth time and saturates at a level dependent on the nucleation conditions.[8,13] As the growth anneal time lengthens, the size of the precipitates increases whilst their density remains approximately constant. A supporting TEM study shows that dislocations and stacking faults surround some of the precipitates for longer growth times.[13] The morphologies of the dominant precipitate type in the samples investigated are summarized in Fig. 1 and densities are plotted in Ref. 8.

[a)]E-mail: k.bothe@isfh.de.
[b)]E-mail: rfalster@memc.it.
[c)]E-mail: john.murphy@materials.ox.ac.uk.

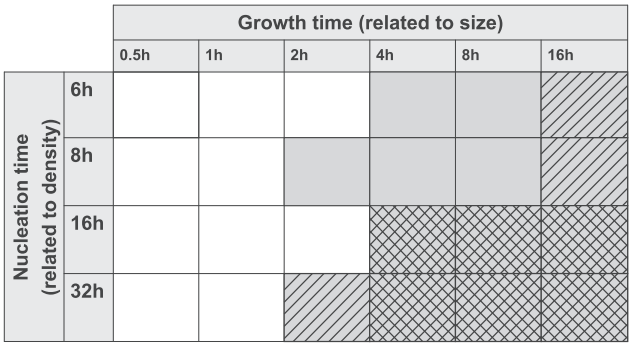

FIG. 1. Matrix of 24 samples containing different morphologies and densities of oxide precipitates. White rectangles ☐ indicate samples predominantly containing unstrained precipitates; grey rectangles ▭ are for those containing predominantly strained precipitates. Hatching indicates the presence of extended defects in addition to the strained precipitates: diagonal lines for dislocations ▨; crossed diagonal lines for stacking faults and dislocations ▧.

For PL measurements, silicon nitride was deposited on both surfaces to provide electronic passivation, resulting in surface recombination velocities below 10 cm/s.[26] PL emission was detected using the set-up described in Ref. 27, which uses an indium gallium arsenide (InGaAs) complementary metal-oxide semiconductor focal plane array. 20 optical band-pass filters with central wavelengths from 1115 to 1690 nm and maximum band widths of 25 to 30 nm allowed spectral selection. All camera-based values reported are area-averaged over $\sim 4 \times 4$ cm^2. Absolute intensities are obtained by scaling these to those made using a diode array spectroradiometer. These calibrated PL measurements are performed by placing the detection unit of the spectroradiometer below the sample, which is homogenously illuminated from the front using an 809 nm gallium arsenide diode laser equipped with a microlens beam homogenizer shaping the fibre output beam to a square flattop with homogeneity of $\pm 5\%$ across the sample area. Exemplarily, Fig. 2 shows the PL spectrum of a sample containing predominantly strained precipitates without surrounding dislocations and stacking faults. While the camera measurements are shown as open squares, the spectroradiometer data are shown as a continuous line. As can be clearly seen, the noise level of the spectroradiometer limits the detection of intensities above 10^{-5} W/m^2/nm. However, the InGaAs camera can be used for intensities down to 10^{-6} W/m^2/nm allowing detection of low intensity sub-bandgap luminescence from oxide precipitates.

A typical PL spectrum is denoted by points in Fig. 2 and shows broad band-to-band emission at 1100 to 1350 nm and a broad sub-bandgap peak at 1480 to 1680 nm centred on ~1600 nm. We analyse our data by integrating the PL signal over these separate wavelength ranges. Fig. 3(a) shows the band-to-band PL decreases with precipitate growth time for each of the nucleation times studied. As the band-to-band PL decreases, Fig. 3(b) shows the appearance and growth of the broad sub-bandgap peak. The band-to-band PL decays approximately exponentially with increasing growth time. The curves used to fit the data in Fig. 3(a) have $1/e$ time constants of 4.8, 2.6, and 1.2 h^{-1} for nucleation times of 6, 8, and 16 h, respectively. The increase in sub-bandgap luminescence in Fig. 3(b) is well described by an initial exponential

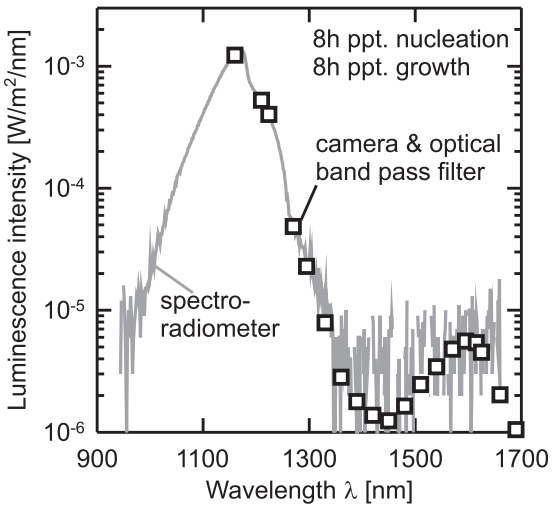

FIG. 2. Spectrally resolved photoluminescence of a surface-passivated silicon sample containing oxide precipitates. Luminescence is detected by an InGaAs camera equipped with different optical band pass filters. Absolute intensities are obtained by scaling the camera data to spectroradiometer measurements.

rise with the same time constants. The decrease in band-to-band recombination is, therefore, balanced by the initial increase in radiative recombination. Fig. 3(b) also shows a sudden decrease in the sub-bandgap PL after a certain

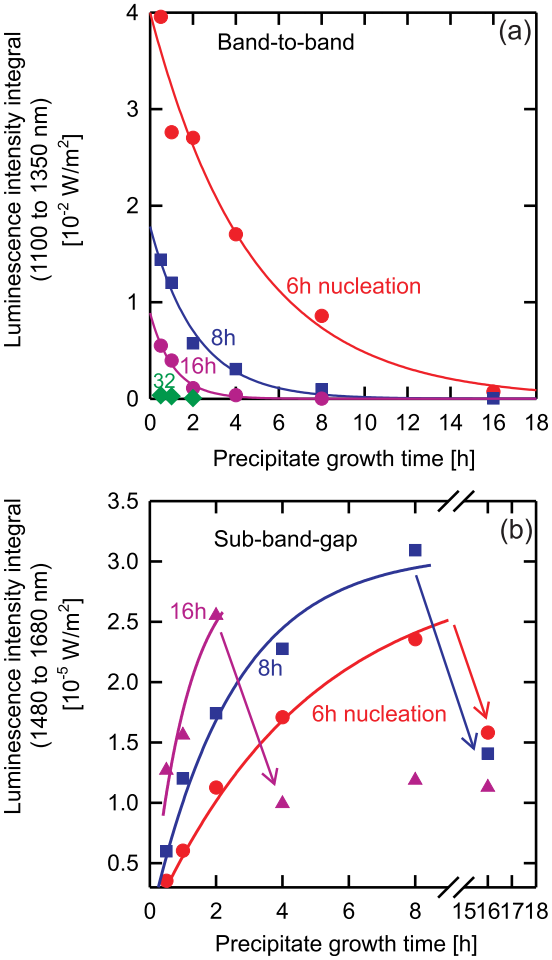

FIG. 3. Wavelength integrated (a) band-to-band and (b) sub-bandgap luminescence intensity as a function of precipitate growth time for different nucleation times.

growth time. The growth time at which this abrupt reduction occurs is dependent upon nucleation time. In samples nucleated for 6 and 8 h, the reduction occurs at 16 h growth time, but in samples nucleated for 16 h, this effect occurs after just 4 h. Fig. 1 shows the growth time at which the reduction in PL signal first occurred was the shortest growth time at which dislocations were observed to have formed around the precipitates. The matrix of samples studied had a limited number of growth time steps, so any difference between the samples nucleated for 6 and 8 h could not be resolved.

The broad sub-bandgap PL peak at ~1600 nm has previously been assigned to oxide precipitates by Kitagawara *et al.*[16] and Tajima *et al.*[3,18] Data in Fig. 3(b) demonstrate that the intensity of this peak relates to precipitate growth and nucleation times and this provides further confirmation of the assignment. For any given nucleation time, the density of unstrained precipitates decreases with growth time as they convert into strained precipitates.[13] Data presented in Fig. 3(b) show an initial increase in sub-bandgap PL with growth time, hence we conclude that unstrained precipitates do not give rise to a detectable sub-bandgap PL signal in wavelength range studied ($\leq$ 1690 nm). For shorter nucleation and growth times, Fig. 4 shows there is a clear correlation between the broad peak at ~1600 nm and the density of strained precipitates. This supports the view that this peak is associated with *strained* oxide precipitates.[3,13,14] Figs. 3(b) and 4 show an abrupt drop in the intensity of sub-bandgap luminescence at a given growth time or density respectively. TEM investigations on the same sample set[13,21] show this reduction correlates exactly with the onset of the dislocations (and in some cases stacking faults) being observed around some of the precipitates (Fig. 1).

Lifetime measurements made on the same sample set show that recombination at oxide precipitates can be parameterised in terms of two Shockley-Read-Hall (SRH) centres at $E_C - 0.08$ eV and $E_V + 0.22$ eV.[10] At room temperature, the state closer to the conduction band has an electron capture coefficient ~1200 times less than that for holes, whereas the state near the valence band has an electron capture coefficient 157 times greater than that for holes. We observed a broad PL peak at ~0.8 eV, which agrees well with the 0.80 eV difference between the SRH centres. To explain the sub-bandgap PL peak observed, we propose the mechanism

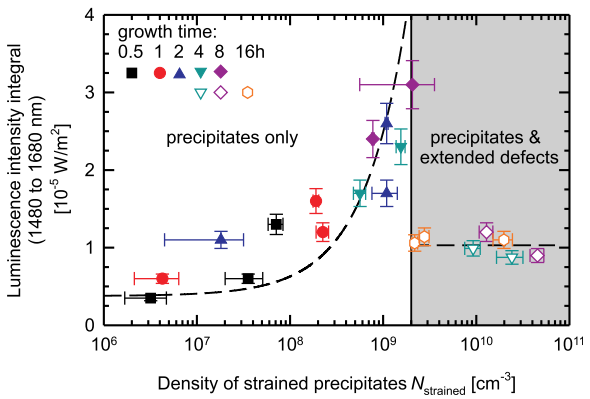

FIG. 4. Integrated sub-bandgap luminescence versus the density of strained oxide precipitates. Open symbols denote specimens in which dislocations and stacking faults were found to surround some precipitates.

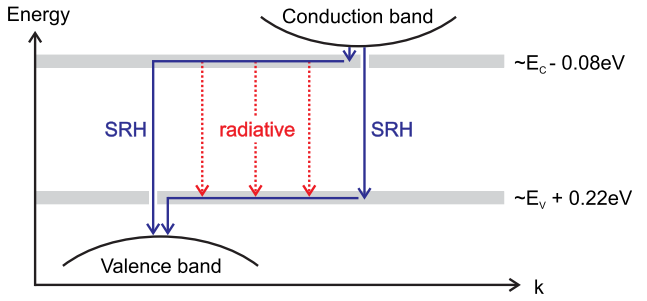

FIG. 5. An energy level diagram to show the possible origin of PL from silicon containing oxide precipitates. Radiative emission is proposed to occur upon electron transitions between bands of defect states associated with the strained precipitates. The same bands also give rise to SRH recombination.

illustrated by Fig. 5. In this model, most recombination occurs via a non-radiative SRH mechanism via the lower energy state with its strong propensity for electron capture or via the upper level with its propensity for holes. The PL emission is proposed to arise from electrons captured by the upper level falling to the lower level and releasing their energy radiatively. We suggest that the broad nature of the PL peak is because the oxide precipitates actually give rise to a band of defect states. The apparently discrete states used to parameterise the lifetime data represent the effective recombination activity of the levels in the bands.

Fig. 4 shows that dislocations and stacking faults around the precipitates reduce radiative emission, but do not eliminate it entirely. Analysis of lifetime data shows (under the assumption that the capture coefficients do not change) the densities of SRH centres per precipitate increase by a factor of 2 to 3 when dislocations and stacking faults surround the precipitates.[10] There is no evidence for additional SRH centres associated with the dislocations and stacking faults, yet it is clear that the presence of these defects reduces the PL emission. We suggest the reduction in PL emission occurs due to increased non-radiative SRH recombination associated with the dislocations and stacking faults. It is possible that small differences between the SRH centres associated with dislocations/stacking faults and the precipitates themselves are not resolvable by lifetime measurement technique.

Monitoring the intensity of sub-bandgap luminescence could be a useful method for process control in oxygen precipitation in silicon wafers. It is known that complete gettering can be achieved by a concentration of strained precipitates as low as ~10^7 cm^{-3}.[28] By monitoring the PL signal, it should be possible to prevent the formation of the dislocations and stacking faults around precipitates which lower carrier lifetime.[8,10] Furthermore, as the formation of oxide precipitates is routine in silicon processing, it may be possible to exploit their weak room temperature light-emitting properties in silicon photonics.[29]

In summary, we have studied room temperature PL in silicon processed to contain oxide precipitates with a variety of morphologies and densities. Unstrained oxide precipitates do not give rise to a detectable PL signal. In samples containing low concentrations of strained precipitates, PL emission mainly occurs via the band-to-band process. A broad room temperature PL peak centred at ~1600 nm is associated with strained oxide precipitates. The conversion of unstrained

precipitates into strained precipitates correlates with an increase in the intensity of this sub-bandgap peak and a corresponding reduction in band-to-band emission. We have proposed a mechanism for the radiative process in terms of a transition between two defect bands. Dislocations and stacking faults around strained oxide precipitates provide a competing non-radiative recombination pathway, which reduces the intensity of the sub-bandgap emission associated with strained oxide precipitates.

We thank D. Gambaro, M. Cornara, and M. Olmo for performing precipitation treatments and characterisation, V. Y. Resnik for TEM analysis, M. Tajima for helpful discussions, and J. P. Hermenau for detailed analysis of measurement equipment and numerous luminescence measurements. J.D.M. holds a Royal Academy of Engineering/EPSRC Research Fellowship.

[1]D. Gilles, E. R. Weber, and S.K. Hahn, Phys. Rev. Lett. **64**, 196 (1990).
[2]H. J. Möller, C. Funke, A. Lawerenz, S. Riedel, and M. Werner, Sol. Energy Mater. Sol. Cells **72**, 403 (2002).
[3]M. Tajima, Y. Iwata, F. Okayama, H. Toyota, H. Onodera, and T. Sekiguchi, J. Appl. Phys. **111**, 113523 (2012).
[4]K. Bothe, K. Ramspeck, D. Hinken, C. Schinke, J. Schmidt, S. Herlufsen, R. Brendel, J. Bauer, J.-M. Wagner, N. Zakharov, and O. Breitenstein, J. Appl. Phys. **106**, 104510 (2009).
[5]J. Haunschild, I. E. Reis, J. Geilker, and S. Rein, Phys. Status Solidi RRL **5**, 199 (2011).
[6]P. K. Kulshreshtha, Y. Yoon, K. M. Youssef, E. A. Good, and G. Rozgonyi, J. Electrochem. Soc. **159**, H125 (2012).
[7]J. Vanhellemont, E. Simoen, A. Kaniava, M. Libzeny, and C. Claeys, J. Appl. Phys. **77**, 5669 (1995).
[8]J. D. Murphy, K. Bothe, M. Olmo, V. V. Voronkov, and R. J. Falster, J. Appl. Phys. **110**, 053713 (2011).
[9]V. Lang, J. D. Murphy, R. J. Falster, and J. J. L. Morton, J. Appl. Phys. **111**, 013710 (2012).
[10]J. D. Murphy, K. Bothe, R. Krain, V. V. Voronkov, and R. J. Falster, J. Appl. Phys. **111**, 113709 (2012).
[11]L. Chen, X. Yu, P. Chen, P. Wang, X. Gu, J. Lu, and D. Yang, Sol. Energy Mater. Sol. Cells **95**, 3148 (2011).
[12]W. Bergholz, M. J. Binns, G. R. Booker, J. C. Hutchison, S. H. Kinder, S. Messoloras, R. C. Newman, R. J. Stewart, and J. G. Wilkes, Philos. Mag. B **59**, 499 (1989).
[13]R. Falster, V. V. Voronkov, V. Y. Resnik, and M. G. Milvidskii, in Proceedings of the Electrochemical Society, High Purity Silicon VIII (2004), Vol. 200405, p. 188.
[14]N. S. Minaev and A. V. Mudryi, Phys. Status Solidi A **68**, 561 (1981).
[15]M. Tajima, J. Cryst. Growth **103**, 1 (1990).
[16]Y. Kitagawara, R. Hoshi, and T. Takenaka, J. Electrochem. Soc. **139**, 2277 (1992).
[17]O. King and D. G. Hall, Phys. Rev. B **50**, 10661 (1994).
[18]M. Tajima, M. Tokita, and M. Warashina, Mater. Sci. Forum **196–201**, 1749 (1995).
[19]S. Ibuka, M. Tajima, H. Takeno, M. Warashina, T. Abe, and K. Nagasaka, Jpn. J. Appl. Phys., Part 2 **36** L494 (1997).
[20]S. Pizzini, M. Guzzi, E. Grilli, and G. Borionetti, J. Phys.: Condens. Matter **12**, 10131 (2000).
[21]E. A. Steinman, A. N. Tereshchenko, V. Ya. Reznik, and R. J. Falster, Phys. Status Solidi A **204**, 2238 (2007).
[22]E. Simoen, R. Loo, C. Claeys, O. De Gryse, P. Clauws, J. Van Landuyt, and O. Lebedev, J. Phys.: Condens. Matter **14**, 13185 (2002).
[23]N. A. Drozdov, A. A. Patrin, and V. D. Tkachev, JETP letters **23**, 597 (1976).
[24]K. F. Kelton, R. Falster, D. Gambaro, M. Olmo, M. Cornara, and P. F. Wei, J. Appl. Phys. **85**, 8097 (1999).
[25]J. D. Murphy and R. J. Falster, Phys. Status Solidi RRL **5**, 370 (2011).
[26]T. Lauinger, J. Schmidt, A. G. Aberle, and R. Hezel, Appl. Phys. Lett. **68**, 1232 (1996).
[27]D. Hinken, C. Schinke, S. Herlufsen, A. Schmidt, K. Bothe, and R. Brendel, Rev. Sci. Instrum. **82**, 033706 (2011).
[28]R. J. Falster, G. R. Fisher, and G. Ferrero, Appl. Phys. Lett. **59**, 809 (1991).
[29]L. Pavesi, J. Phys.: Condens. Matter **15**, R1169 (2003).